

A scaling law of multilevel selection on a continuous trait

Nobuto Takeuchi*

*School of Biological Sciences, the University of Auckland,
Private Bag 92019, 1142 Auckland, New Zealand and
Research Center for Complex Systems Biology, Universal Biology Institute,
the University of Tokyo, Komaba 3-8-1, Meguro-ku, Tokyo 153-8902, Japan*

Namiko Mitarai†

*The Niels Bohr Institute, University of Copenhagen,
Blegdamsvej 17, Copenhagen, 2100-DK, Denmark and
Research Center for Complex Systems Biology, Universal Biology Institute,
the University of Tokyo, Komaba 3-8-1, Meguro-ku, Tokyo 153-8902, Japan*

Kunihiko Kaneko‡

*Graduate School of Arts and Sciences, the University of Tokyo,
Komaba 3-8-1, Meguro-ku, Tokyo 153-8902, Japan and
Research Center for Complex Systems Biology, Universal Biology Institute,
the University of Tokyo, Komaba 3-8-1, Meguro-ku, Tokyo 153-8902, Japan*

(Dated: May 15, 2022)

Living systems are hierarchically structured, whereby replicating components are grouped into reproducing collectives; e.g., organelles are grouped into cells; cells, into multicellular organisms; and multicellular organisms, into colonies. We consider how such hierarchically-structured replicator systems evolve along a continuum—between cooperation and cheating. Cooperation is selected through competition among collectives, whereas cheating is selected through competition among replicating components within collectives. We determine how the evolution depends on the number of replicating components per collective (N) and the mutation rate of replicating components (m). We demonstrate a scaling relation that holds when selection for cooperation exactly balances out selection for cheating: $N \propto m^{-\alpha}$, where α (> 0) increases with selection strength. Increasing N or m drives the system towards a phase where cheating evolves, and the above scaling relation separates this phase from that where cooperation evolves. We develop a simple theory that can account for this scaling relation using moment evolution equations and clarify the limit of applicability of the theory using time-backward observation.

A fundamental feature of living systems is hierarchical organization, in which replicating components are grouped into reproducing collectives [1]. For example, replicating molecules are grouped into protocells [2]; organelles, such as mitochondria, are grouped into cells [3]; cells are grouped into multicellular organisms [4]; and multicellular organisms are grouped into colonies [5, 6].

Such hierarchical organization hinges on cooperation among components, the group action that increases collective-level fitness at the cost of inhibiting the self-replication of individual components. For example, in protocells, molecules catalyze chemical reactions to facilitate the growth of the cell at the cost of inhibiting themselves from serving as templates for replication, the expense that arises from a trade-off between serving as catalysts and serving as templates [7, 8]. Likewise, in multicellular organisms, cells perform somatic functions beneficial to the whole organism, such as defense and locomotion, at the cost of reducing cell proliferation due to different trade-offs [4, 9].

Cooperation, however, entails the risk of invasion by cheaters, i.e., components that avoid cooperation and instead replicate themselves to the detriment of the collective. For example, parasitic templates replicate to the detriment of protocells [10, 11], and cancer cells proliferate to the detriment of multicellular organisms [12]. Cheating is favored by selection *within* collectives because it increases the relative fitness of components within collectives. Contrariwise, cooperation is favored by selection *among* collectives because it increases fitness at the level of collectives—hence, conflicting multilevel selection.

Whether cheating or cooperation predominates depends on the balance between evolution driven by within-collective selection and evolution driven by among-collective selection [13]. Shifting this balance exerts profound impacts on evolutionary outcomes. For example, shifting this balance towards within-collective evolution can induce spontaneous symmetry breaking of replicating molecules in protocells, whereby the molecules differentiate into genomes and enzymes, establishing the central dogma of molecular biology [14]. It is thus important to determine how this balance depends on parameters of population dynamics, such as the number of replicating components per collective and the mutation rate of the

* nobuto.takeuchi@auckland.ac.nz

† mitarai@nbi.dk

‡ kaneko@complex.c.u-tokyo.ac.jp

components.

Although there are many studies modeling multilevel selection on discrete traits [11, 15–22], a relatively few have modeled it on continuous traits [23–25]. However, many traits of biological importance, such as catalytic activities of molecules and growth rates of cells [26–28], exhibit continuous variation because they are influenced by a number of factors [29].

Here we investigate the simplest model of multilevel selection on a continuous trait. Our model is an extension of the Wright-Fisher model [30], a standard model of population genetics, to allow for multilevel selection. The model consists of replicators grouped into collectives that can grow and divide. Each replicator possesses a continuous heritable trait representing the amount of public good it provides to the collective it belongs to (e.g., it represents the amount of chemical catalysis a replicating molecule provides to the protocell). Using the model, we determine how the evolution of public good provision depends on the maximum number of replicators per collective (N), the mutation rate of replicators (m), and selection strength (s). We first confirm an earlier result that increasing N or m inhibits the evolution of public good provision because it accelerates within-collective evolution relative to among-collective evolution [31, 32]. Our main result is that when within-collective evolution and among-collective evolution exactly balance each other out, the following scaling relation holds: $N \propto m^{-\alpha}$, where α (> 0) increases with s . This relation differs from that reported for multilevel selection on discrete traits: $N \propto m^{-1}$ [17].

Let us consider a population of M replicators grouped into collectives, each consisting of at most N replicators (Fig. 1). Replicator j in collective i is assigned a continuous trait k_{ij} representing the amount of public good it provides to collective i . Replicators are assumed to face a trade-off between public good provision and self-replication. Thus, the fitness of individual replicators w_{ij} decreases with individual trait k_{ij} , whereas the collective-level fitness of replicators $\langle w_{i\tilde{j}} \rangle$ increases with collective-level trait $\langle k_{i\tilde{j}} \rangle$, where $\langle x_{i\tilde{j}} \rangle$ is x_{ij} averaged over replicators in collective i (i.e., x_{ij} is averaged over the index marked with a tilde). For simplicity, we assume that the strengths of selection within and among collectives, defined as

$$s_w = -\frac{\partial \ln w_{ij}}{\partial k_{ij}} \quad \text{and} \quad s_a = \frac{\partial \ln \langle w_{i\tilde{j}} \rangle}{\partial \langle k_{i\tilde{j}} \rangle}, \quad (1)$$

respectively, depend very weakly on k_{ij} . Accordingly, we used the following fitness function for simulations:

$$w_{ij} = e^{s_a \langle k_{i\tilde{j}} \rangle} \frac{e^{-s_w k_{ij}}}{\langle e^{-s_w k_{i\tilde{j}}} \rangle}, \quad (2)$$

where we set $s_w = s_a = s$.

The state of the model is updated in discrete time (Fig. 1). In each generation, M replicators are sampled

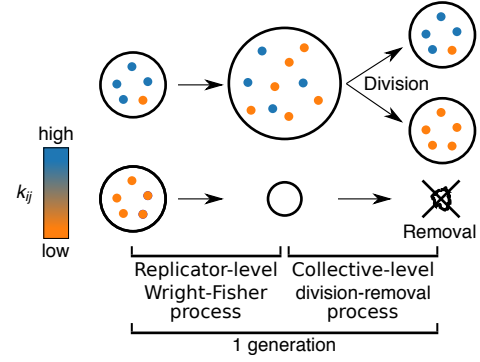


FIG. 1. Schematic of model. Replicators (dot) are grouped into collectives (circles). k_{ij} represents amount of public good replicators provides within collectives.

with replacement from replicators of the previous generation with probabilities proportional to w_{ij} , as in the Wright-Fisher process [30]. During the sampling, a replicator inherits i (group identity) and k_{ij} from its parental replicator. The value of k_{ij} , however, can mutate to $k_{ij} + \delta_k$ with a probability m , where δ_k is sampled from a Gaussian distribution with mean 0 and variance σ . After the sampling, collectives with more than N replicators are randomly divided into two, and those with no replicators removed.

By simulating the above model, we measured the rate of change of $\langle k_{i\tilde{j}} \rangle$, where $\langle x_{i\tilde{j}} \rangle$ is x_{ij} averaged over all replicators, at steady states as a function of m and N [33]. The result indicates the existence of two phases, where $\langle k_{i\tilde{j}} \rangle$ either increases or decreases through evolution (Fig. 2). The phases are demarcated by a scaling relation $N \propto m^{-\alpha}$, where α increases with s (Fig. 3)—i.e., the evolution of $\langle k_{i\tilde{j}} \rangle$ depends on m increasingly strongly as s increases. These results extend those previously obtained with specific models of protocells [31, 32].

Next, we present a theory that can account for $N \propto m^{-\alpha}$ under the assumption that $s \ll 1$. Although such a theory could in principle be built by calculating the dynamics of the frequency distribution of k_{ij} , for simplicity, we instead calculate the dynamics of the moments of this distribution. A change of $\langle k_{i\tilde{j}} \rangle$ per generation is expressed by Price's equation as follows [34]:

$$\Delta \langle k_{i\tilde{j}} \rangle = \langle w_{i\tilde{j}} \rangle^{-1} \text{cov}_{i\tilde{j}}[\langle w_{i\tilde{j}} \rangle, \langle k_{i\tilde{j}} \rangle] + \langle w_{i\tilde{j}} \rangle^{-1} \mathbb{E}_{i\tilde{j}}[\text{cov}_{i\tilde{j}}[w_{ij}, k_{ij}]], \quad (3)$$

where $\text{cov}_{i\tilde{j}}[x_i, y_i]$ is covariance between x_i and y_i over collectives, $\text{cov}_{i\tilde{j}}[x_{ij}, y_{ij}]$ is covariance between x_{ij} and y_{ij} over replicators in collective i , and $\mathbb{E}_{i\tilde{j}}[x_i]$ is x_i averaged over collectives. Expanding Eq. (3) around $k_{ij} = \langle k_{i\tilde{j}} \rangle$ and $\langle k_{i\tilde{j}} \rangle = \langle k_{i\tilde{j}} \rangle$ [35], we obtain

$$\Delta \langle k_{i\tilde{j}} \rangle \approx s_a v_a - s_w v_w, \quad (4)$$

where v_a is the variance of $\langle k_{i\tilde{j}} \rangle$ among collectives, and v_w is the average variance of k_{ij} among replicators within a collective.

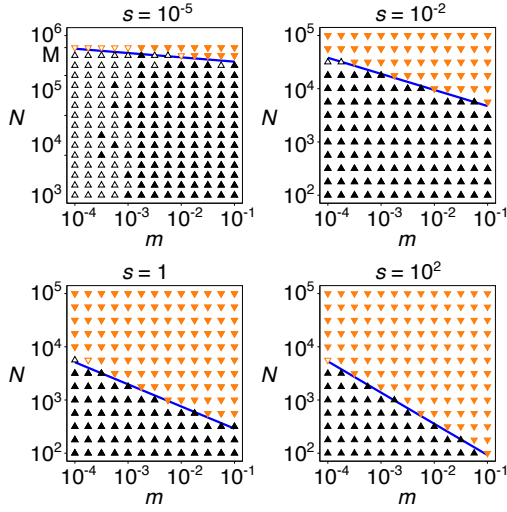


FIG. 2. Phase diagrams ($M = 5 \times 10^5$ and $\sigma = 10^{-4}$). Symbols have following meaning: $\Delta\langle k_{ij} \rangle > 3 \times 10^{-7}$ (filled triangle up); $\Delta\langle k_{ij} \rangle < -3 \times 10^{-7}$ (filled triangle down); RHS of Eq. (3) measured in simulations is positive (open triangle up) or negative (open triangle down), where $|\Delta\langle k_{ij} \rangle| < 3 \times 10^{-7}$. Lines are estimated phase boundaries. See also Footnote [33].

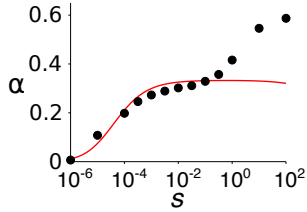


FIG. 3. Scaling exponents of phase boundaries ($M = 5 \times 10^5$ and $\sigma = 10^{-4}$). Dots are simulation results. Line is prediction by Eq. (11).

Equation (4) indicates that the phase boundary $\Delta\langle k_{ij} \rangle = 0$ depends on v_w and v_a . To calculate v_w and v_a , we first consider a neutral case where $s_a = s_w = 0$. Let the total variance be $v_t = v_a + v_w$. In each generation, M replicators are randomly sampled from replicators of the previous generation with mutation. The sampling decreases the variance by a factor of $1 - M^{-1}$ [36], while mutation increases it by $m\sigma$. Therefore, the variance of the next generation is

$$v'_t = (1 - M^{-1})(v_t + m\sigma). \quad (5)$$

Likewise, the change of v_w per generation can be calculated. To enable this calculation, we assume that all collectives always consist of $\beta^{-1}N$ replicators, where β is a constant [37]. Randomly sampling $\beta^{-1}N$ replicators from a collective with mutation changes v_w to

$$v'_w = (1 - \beta N^{-1})(v_w + m\sigma). \quad (6)$$

Since $v'_a = v'_t - v'_w$, we obtain

$$v'_a = (1 - M^{-1})v_a + (\beta N^{-1} - M^{-1})(v_w + m\sigma). \quad (7)$$

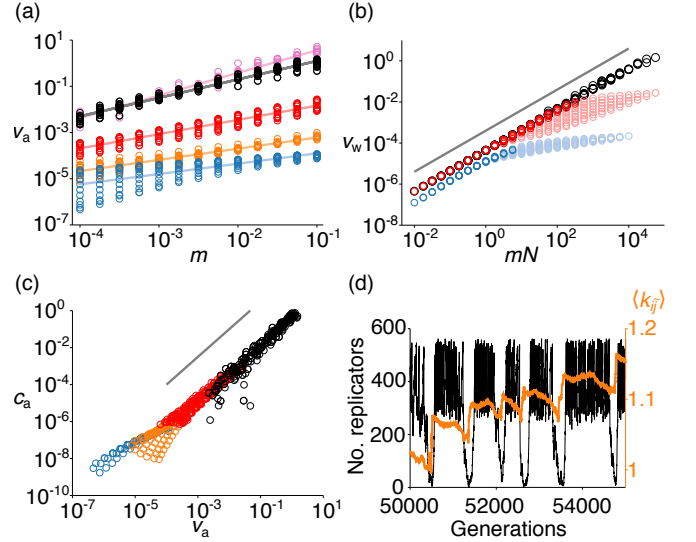


FIG. 4. Testing theory by simulations ($M = 5 \times 10^5$, $\sigma = 10^{-4}$). (a) Circles are simulation results: $s = 10^{-6}$ (pink), 10^{-5} (black), 10^{-2} (red), 1 (orange), 10^2 (blue). Lines are least squares regression: $v_a \propto m^\eta$, where $\eta = 0.98$ (pink), 0.8 (black), 0.62 (red), 0.48 (orange), 0.45 (blue). (b) Circles are simulation results: $s = 10^{-5}$ (black), 10^{-2} (red), 10^2 (blue). For $s = 10^{-2}$ or 10^2 , lighter (or darker) colors indicate $\Delta\langle k_{ij} \rangle < 0$ (or > 0 , respectively). Line is $v_w \propto mN$, as predicted by Eq. (11). (c) Circles are simulation results: $s = 10^{-5}$ (black), 10^{-2} (red), 10^2 (blue). Line is $c_w \propto v_w^{3/2}$, as postulated in Eq. (10). (d) Dynamics of common ancestors of collectives: number of replicators per collective (black) and $\langle k_{ij} \rangle$ (orange). $s = 1$, $N = 562$, and $m = 0.01$.

Next, we consider the effect of selection on v_a . Using Price's equation, we can express the change of v_a per generation due to selection as follows [38]:

$$\begin{aligned} \Delta_s v_a = & \langle w_{ij} \rangle^{-1} \text{cov}_i \left[\langle w_{ij} \rangle, (\langle k_{ij} \rangle - \langle \langle k_{ij} \rangle \rangle)^2 \right] \\ & - \langle w_{ij} \rangle^{-2} \left\{ \text{cov}_i \left[\langle w_{ij} \rangle, \langle k_{ij} \rangle \right] \right\}^2. \end{aligned} \quad (8)$$

Expanding Eq. (8) around $\langle k_{ij} \rangle = \langle \langle k_{ij} \rangle \rangle$, we obtain

$$\Delta_s v_a \approx s_a c_a - (s_a v_a)^2 \quad (9)$$

where c_a is the third central moment of $\langle k_{ij} \rangle$.

Based on the dimensional argument, we postulate that

$$c_a = -\gamma v_a^{3/2}, \quad (10)$$

where γ is a constant. Combining Eqs. (6), (7), (9) and (10), we obtain

$$\begin{aligned} \Delta v_w & \approx -\beta N^{-1} v_w + (1 - \beta N^{-1}) m\sigma \\ \Delta v_a & \approx -M^{-1} v_a + (\beta N^{-1} - M^{-1})(v_w + m\sigma) \\ & \quad - \gamma s_a v_a^{3/2}, \end{aligned} \quad (11)$$

where we have assumed that $s_a \ll 1$ and that $\beta N^{-1} v_w \gg$

$s_w|c_w|$. At a steady state, Eq. (11) implies that

$$v_w \approx \beta^{-1} N m \sigma$$

$$v_a \approx \begin{cases} M m \sigma & \text{if } s_a \ll (\gamma \sqrt{m \sigma} M^{2/3})^{-1} \\ [m \sigma / (\gamma s_a)]^{2/3} & \text{if } s_a \gg (\gamma \sqrt{m \sigma} M^{2/3})^{-1}, \end{cases} \quad (12)$$

where $\gamma > 0$ is demanded, and $M \gg \beta^{-1} N \gg 1$ assumed. Equation (12) shows that v_a is independent of N , which can be understood as follows. According to Eq. (7), the increase of v_a per generation is approximately proportional to $N^{-1} v_w$, where $v_w \propto N m$ at steady states, so that N cancels out. This cancellation is similar to that occurring in the rate of neutral molecular evolution, which is also independent of population size [39].

To examine the validity of Eq. (11), we measured v_a , v_w , and c_a through simulations (Fig. 4). The results show that $v_a \propto m N$ for a very small value of s_a (viz., 10^{-6}) in agreement with Eq. (12) (Fig. 4a). Moreover, $v_w \propto m N$ as predicted by Eq. (12) (Fig. 4b), except for cases where $\Delta \langle k_{ij} \rangle < 0$ (this deviation will be discussed later). Finally, $c_a \propto v_a^{3/2}$ for $s \ll 1$ as postulated in Eq. (10) (Fig. 4c). Taken together, these results support the validity of Eq. (11).

To further validate Eq. (11), we calculated the scaling exponent α . For extreme values of s , Eq. (12) implies that $N \propto m^{-\alpha}$ if $\Delta \langle k_{ij} \rangle = 0$, where

$$\alpha \approx 0 \quad \text{if } s_a \ll (\gamma \sqrt{m \sigma} M^{2/3})^{-1} \quad \text{or} \quad (13)$$

$$\alpha \approx 1/3 \quad \text{if } s_a \gg (\gamma \sqrt{m \sigma} M^{2/3})^{-1}.$$

For intermediate values of s , we numerically calculated the values of m and N for which Eq. (11) is at steady states using the values of β and γ estimated from Fig. 4bc (viz., $\beta = 0.45$ and $\gamma = 0.26$). These values of m and N were used to calculate α through the least squares regression of $N \propto m^{-\alpha}$ for $m \in [10^{-4}, 10^{-1}]$. The results qualitatively agree with the simulation results for $s < 1$ (Fig. 3), supporting the validity of Eq. (11).

In addition, we note that the postulate in Eq. (10) is also supported by previous studies calculating the evolution of a continuous trait (viz., fitness) subject to single-level selection [40, 41]. These studies show that fitness increases through evolution at a rate proportional to the two-third power of the mutation rate. This is consistent with Eq. (11) and, hence, Eq. (10), as follows. Following Ref. [40], let us assume single-level selection ($s_w = 0$) and a very large population ($M \rightarrow \infty$) in Eqs. (4) and (11). Then, the equations imply that logarithmic fitness, $\ln \langle w_{ij} \rangle \propto \langle k_{ij} \rangle$, increases at a rate proportional to $m^{2/3}$ (Supplemental Material Fig. S1). Moreover, using the result of Ref. [40], we can estimate the value of γ as about

0.25 (Supplemental Material), which roughly matches the value measured in our model (viz. 0.26).

Finally, to clarify why Eq. (11) deviates from the simulation results for $s \gtrsim 1$ or $\Delta \langle k_{ij} \rangle < 0$, we tracked the genealogy of collectives backward in time to observe the common ancestors of all collectives. Figure 4d shows the dynamics of $\langle k_{ij} \rangle$ and the number of replicators in these ancestors along their line of descent. The results indicate that the model displays a phenomenon previously described as *evolutionarily stable disequilibrium* (ESD, for short) [31]. Briefly, the collectives constantly oscillate between growing and shrinking phases (Fig. 4d). During the growing phase, the collectives continually grow and divide, and their $\langle k_{ij} \rangle$ values gradually decline through within-collective evolution, a decline that eventually puts the collectives to a shrinking phase. In the shrinking phase, the collectives steadily shrink; however, their $\langle k_{ij} \rangle$ values abruptly jump at the end of the phase, a transition that brings the collectives back to the growing phase. This sudden increase of $\langle k_{ij} \rangle$ is due to random genetic drift induced by severe within-collective population bottlenecks. Although such an increase is an extremely rare event, it is always observed in the common ancestors because these ancestors are the survivors of among-collective selection, which favors high $\langle k_{ij} \rangle$ values [31, 32].

ESD breaks the assumption that all collectives always consist of $\beta^{-1} N$ replicators, accounting for the failure of Eq. (11). This inference is attested by the fact that ESD occurs for $s \gtrsim 1$ (Fig. 4d) or $\Delta \langle k_{ij} \rangle < 0$ (Supplemental Material Fig. S2). In addition, v_a and c_a constantly oscillate for $s \geq 1$ (Supplemental Material Fig. S3), in which case it is questionable to consider a steady-state solution such as Eq. (12).

In summary, we studied an extension of the Wright-Fisher model allowing for multilevel selection, discovered a novel scaling relation $N \propto m^{-\alpha}$, developed a simple theory that can explain this relation, and clarified the limit of validity of the theory by demonstrating ESD. An important issue to address for future research is to develop a theory allowing for ESD to calculate $\Delta \langle k_{ij} \rangle$.

Capturing the essence of multilevel selection, the model presented above is likely to have broad applicability. It is generally relevant for the evolution of cooperation in replicators grouped into reproducing collectives, e.g., symbionts, organelles, or genetic elements grouped into cells [3], cells grouped into multicellular organisms [4], or any system immediately after a major evolutionary transition [1].

We thank Omri Barak for discussion and acknowledge the contribution of NeSI to the results of this research. This research was supported by the University of Auckland computational biology theme fund and JSPS KAKENHI Grant Number 15H05746, 17H06386.

- [2] G. F. Joyce and J. W. Szostak, Protocells and RNA self-replication, *Cold Spring Harb Perspect Biol* **10**, a034801 (2018).
- [3] A. Burt and R. Trivers, *Genes in Conflict: The Biology of Selfish Genetic Elements* (Belknap Press, Cambridge, MA, 2006).
- [4] L. W. Buss, *The Evolution of Individuality* (Princeton University Press, Princeton, NJ, 1987).
- [5] N. B. Davies, J. R. Krebs, and S. A. West, Altruism and conflict in the social insects, in *An Introduction to Behavioural Ecology* (Wiley-Blackwell, West Sussex, UK, 2012) 4th ed., Chap. 13, pp. 307–333.
- [6] L. Gershwin, M. Lewis, K. Gowlett-Holmes, and R. Kloser, The Siphonophores, in *Pelagic Invertebrates of South-Eastern Australia: A Field Reference Guide. Version 1.1*, edited by L.-a. Gershwin (CSIRO Marine and Atmospheric Research, Hobart, 2014).
- [7] P. M. Durand and R. E. Michod, Genomics in the light of evolutionary transitions, *Evolution* **64**, 1533 (2010).
- [8] N. A. Ivica, B. Obermayer, G. W. Campbell, S. Rajamani, U. Gerland, and I. A. Chen, The paradox of dual roles in the RNA World: Resolving the conflict between stable folding and templating ability, *J Mol Evol* **77**, 55 (2013).
- [9] D. L. Kirk, *Volvox: Molecular-Genetic Origins of Multicellularity and Cellular Differentiation* (Cambridge, U.K., Cambridge, U.K., 1998).
- [10] Y. Bansho, T. Furubayashi, N. Ichihashi, and T. Yomo, Host-parasite oscillation dynamics and evolution in a compartmentalized RNA replication system., *Proc Nat Acad Sci USA* **113**, 4045 (2016).
- [11] A. Blokhuis, D. Lacoste, P. Nghe, and L. Peliti, Selection dynamics in transient compartmentalization, *Phys Rev Lett* **120**, 158101 (2018).
- [12] M. Greaves and C. C. Maley, Clonal evolution in cancer, *Nature* **481**, 306 (2012).
- [13] E. G. Leigh, The group selection controversy, *J Evol Biol* **23**, 6 (2010).
- [14] N. Takeuchi and K. Kaneko, The origin of the central dogma through conflicting multilevel selection, *Proc R Soc B* **286**, 20191359 (2019).
- [15] D. S. Wilson, A theory of group selection, *Proc Nat Acad Sci USA* **72**, 143 (1975).
- [16] K. Aoki, A condition for group selection to prevail over counteracting individual selection, *Evolution* **36**, 832 (1982).
- [17] M. Kimura, Diffusion model of population genetics incorporating group selection, with special reference to an altruistic trait, in *Stochastic Processes and their Applications*, edited by K. Ito and T. Hida (Springer, Berlin, 1986) pp. 101–118.
- [18] E. Szathmary and L. Demeter, Group selection of early replicators and the origin of life, *J Theor Biol* **128**, 463 (1987).
- [19] A. Traulsen and M. A. Nowak, Evolution of cooperation by multilevel selection, *Proc Nat Acad Sci USA* **103**, 10952 (2006).
- [20] B. Simon, J. A. Fletcher, and M. Doebeli, Towards a general theory of group selection, *Evolution* **67**, 1561 (2013).
- [21] J. F. Fontanari and M. Serva, Nonlinear group survival in Kimura’s model for the evolution of altruism, *Math Biosci* **249**, 18 (2014).
- [22] D. B. Cooney, The replicator dynamics for multilevel selection in evolutionary games, *J Math Biol* **79**, 101 (2019).
- [23] M. Slatkin and M. J. Wade, Group selection on a quantitative character, *Proc Nat Acad Sci USA* **75**, 3531 (1978).
- [24] E. G. Leigh, When does the good of the group override the advantage of the individual?, *Proc Nat Acad Sci USA* **80**, 2985 (1983).
- [25] P. Bijma, W. M. Muir, and J. A. Van Arendonk, Multilevel selection 1: Quantitative genetics of inheritance and response to selection, *Genetics* **175**, 277 (2007).
- [26] L. Jaeger, M. C. Wright, and G. F. Joyce, A complex ligase ribozyme evolved in vitro from a group I ribozyme domain, *Proc Nat Acad Sci USA* **96**, 14712 (1999).
- [27] A. D. Pressman, Z. Liu, E. Janzen, C. Blanco, U. F. Muller, G. F. Joyce, R. Pascal, and I. A. Chen, Mapping a systematic ribozyme fitness landscape reveals a frustrated evolutionary network for self-aminoacylating RNA, *J Am Chem Soc* **141**, 6213 (2019).
- [28] D. E. Dykhuizen and A. M. Dean, Enzyme activity and fitness: Evolution in solution, *Trends Ecol Evol* **5**, 257 (1990).
- [29] D. S. Falconer and T. F. Mackay, *Introduction to Quantitative Genetics*, 4th ed. (Pearson Education Limited, Essex, England, 1996).
- [30] W. J. Ewens, *Mathematical Population Genetics* (Springer New York, New York, NY, 2004).
- [31] N. Takeuchi, K. Kaneko, and P. Hogeweg, Evolutionarily stable disequilibrium: endless dynamics of evolution in a stationary population, *Proc R Soc B* **283**, 20153109 (2016).
- [32] N. Takeuchi, P. Hogeweg, and K. Kaneko, The origin of a primordial genome through spontaneous symmetry breaking, *Nat Commun* **8**, 250 (2017).
- [33] $\Delta\langle\langle k_{ij} \rangle\rangle$ was estimated from slopes of the least squares regression of $\langle\langle k_{ij} \rangle\rangle$ against time. The estimates were unreliable if $|\Delta\langle\langle k_{ij} \rangle\rangle| < 3 \times 10^{-7}$ due to a limitation of simulations, in which case the RHS of Eq. (3) was used as a proxy for $\Delta\langle\langle k_{ij} \rangle\rangle$. Phase boundaries were estimated as follows. The zeros of the RHS of Eq. (3) (or those of $\Delta\langle\langle k_{ij} \rangle\rangle$ if $s \geq 10$) were estimated with quadratic polynomial interpolation with respect to N from three simulation points around a phase boundary for each m value. The estimated zeros were used to obtain a phase boundary through the least squares regression of $N \propto m^{-\alpha}$.
- [34] G. R. Price, Extension of covariance selection mathematics, *Ann Hum Genet* **35**, 485 (1972).
- [35] Y. Iwasa, A. Pomiankowski, and S. Nee, The evolution of costly mate preferences II. The ‘handicap’ principle, *Evolution* **45**, 1431 (1991).
- [36] In general, sample variance of sample size n is smaller than population variance by a factor of $1 - n^{-1}$.
- [37] This assumption becomes invalid if $s \gtrsim 1$ as will be describe later.
- [38] X.-S. Zhang and W. G. Hill, Change and maintenance of variation in quantitative traits in the context of the Price equation, *Theor Popul Biol* **77**, 14 (2010).
- [39] M. Kimura, Evolutionary rate at the molecular level, *Nature* **217**, 624 (1968).
- [40] L. S. Tsimring, H. Levine, and D. A. Kessler, RNA virus evolution via a fitness-space model, *Phys Rev Lett* **76**, 4440 (1996).
- [41] O. Hallatschek, The noisy edge of traveling waves, *Proc Nat Acad Sci USA* **108**, 1783 (2011).

Supplemental materials: A scaling law of multilevel selection on a continuous trait

Nobuto Takeuchi*

*School of Biological Sciences, the University of Auckland,
Private Bag 92019, 1142 Auckland, New Zealand and
Research Center for Complex Systems Biology, Universal Biology Institute,
the University of Tokyo, Komaba 3-8-1, Meguro-ku, Tokyo 153-8902, Japan*

Namiko Mitarai†

*The Niels Bohr Institute, University of Copenhagen,
Blegdamsvej 17, Copenhagen, 2100-DK, Denmark and
Research Center for Complex Systems Biology, Universal Biology Institute,
the University of Tokyo, Komaba 3-8-1, Meguro-ku, Tokyo 153-8902, Japan*

Kunihiko Kaneko‡

*Graduate School of Arts and Sciences, the University of Tokyo,
Komaba 3-8-1, Meguro-ku, Tokyo 153-8902, Japan and
Research Center for Complex Systems Biology, Universal Biology Institute,
the University of Tokyo, Komaba 3-8-1, Meguro-ku, Tokyo 153-8902, Japan*

* nobuto.takeuchi@auckland.ac.nz

† mitarai@nbi.dk

‡ kaneko@complex.c.u-tokyo.ac.jp

ESTIMATION OF γ

Tsimring et al. [1] have investigated the time evolution of the probability density $p(r, t)$ of fitness r subject to mutation and selection. In this section, we show that the results of Tsimring et al. [1] imply $C \approx -0.25V^{3/2}$, where C and V are the variance and the third central moment of $p(r, t)$, respectively. This implication is consistent with our postulate $c_a = -\gamma v_a^{3/2}$ made in Eq. (10) of the main text, where γ was measured to be about 0.25 through simulations.

Tsimring et al. [1] have considered the following equation, which describes the time evolution of $p(r, t)$:

$$\frac{\partial}{\partial t} p(r, t) = \theta(p - p_c) (r - \langle r \rangle) p(r, t) + D \frac{\partial^2}{\partial r^2} p(r, t), \quad (1)$$

where $\theta(x)$ is the Heaviside step function, and $\langle r \rangle$ is the average fitness defined as

$$\langle f(r) \rangle = \int_{-\infty}^{\infty} f(r) p(r, t) dr,$$

and D is a diffusion constant. The first term on the RHS of Eq. (1) describes the effect of selection; the second term, that of mutation. The Heaviside step function accounts for the fact that the probability density $p(r, t)$ must exceed a small threshold density p_c to grow because the size of a population is not infinite in reality. Tsimring et al. have shown that Eq. (1) allows a traveling-wave solution, in which the peak of the density travels toward higher values of r , while maintaining a pulse-like shape, at a steady-state speed (denoted by v)

$$v = cD^{2/3}, \quad (2)$$

where the value of c depends weakly on p_c and is around 4 in a wide range of p_c [1].

Multiplying both sides of Eq. (1) with r or $(r - \langle r \rangle)^2$ and integrating over the whole range, we get

$$\frac{d}{dt} \langle r \rangle = V - \epsilon_1, \quad (3)$$

$$\frac{d}{dt} V = C - \epsilon_2 + 2D, \quad (4)$$

where V , C , ϵ_1 , and ϵ_2 are defined as follows:

$$V = \langle (r - \langle r \rangle)^2 \rangle, \quad (5)$$

$$C = \langle (r - \langle r \rangle)^3 \rangle, \quad (6)$$

$$\epsilon_1 = \langle \theta(p_c - p) (r - \langle r \rangle)^2 \rangle, \quad (7)$$

$$\epsilon_2 = \langle \theta(p_c - p) (r - \langle r \rangle)^3 \rangle. \quad (8)$$

In obtaining Eqs. (3) and (4), we have assumed that the surface terms go to zero as $r \rightarrow \pm\infty$; i.e., $\lim_{r \rightarrow \pm\infty} P(r, t) = 0$, $\lim_{r \rightarrow \pm\infty} rP(r, t) = 0$, $\lim_{r \rightarrow \pm\infty} r \frac{\partial p}{\partial r} = 0$, and $\lim_{r \rightarrow \pm\infty} r^2 \frac{\partial p}{\partial r} = 0$.

For a traveling-wave solution of Eq. (1) with a constant speed v and shape, Eq. (3) implies

$$v = V - \epsilon_1. \quad (9)$$

From Eqs. (2) and (9), we get

$$D = \left(\frac{V - \epsilon_1}{c} \right)^{3/2}. \quad (10)$$

Since v and ϵ_1 are constant, Eq. (9) implies $dV/dt = 0$. Thus, Eq. (4) implies

$$C = -2D + \epsilon_2. \quad (11)$$

Equations (10) and (11) imply

$$C = -2 \left(\frac{V - \epsilon_1}{c} \right)^{3/2} + \epsilon_2 \approx -2c^{-3/2} V^{3/2},$$

where we have assumed $\epsilon_1 \ll V$ and $\epsilon_2 \ll V$ to obtain the last term. Since c is about 4 according to Tsimring et al. [1], we get

$$C \approx -0.25V^{3/2}.$$

SUPPLEMENTARY FIGURES

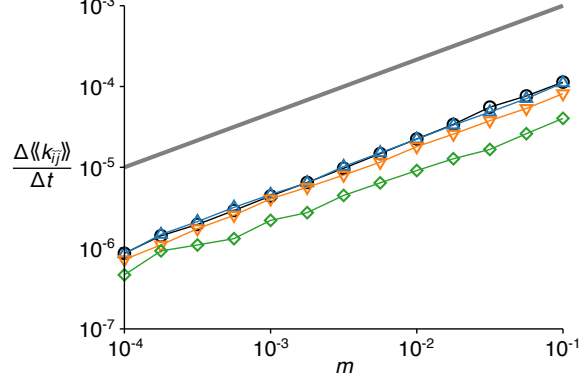


FIG. S1. The rate of logarithmic fitness increase as a function of mutation rate measured through simulations ($s = 10^{-3}$, $M = 5 \times 10^5$ and $\sigma = 10^{-4}$). The fitness is defined as follows: $w_{ij} = e^{s \langle k_{ij} \rangle}$ (i.e., $s_w = 0$ and $s_a = s$). Symbols have the following meaning: $N = 10^2$ (black circles); $N = 10^3$ (blue triangle up); $N = 10^4$ (orange triangle down); $N = 10^4$ (green diamond). Line is $\Delta \langle k_{ij} \rangle / \Delta t \propto m^{2/3}$, as predicted by Eq. (11) in main text. This figure confirms that $\Delta \langle k_{ij} \rangle \propto m^{2/3}$ in agreement with Ref. [1]. Note also that $\Delta \langle k_{ij} \rangle$ is roughly independent of N , which is consistent with the prediction of Eq. (12) in main text that v_a is independent of N .

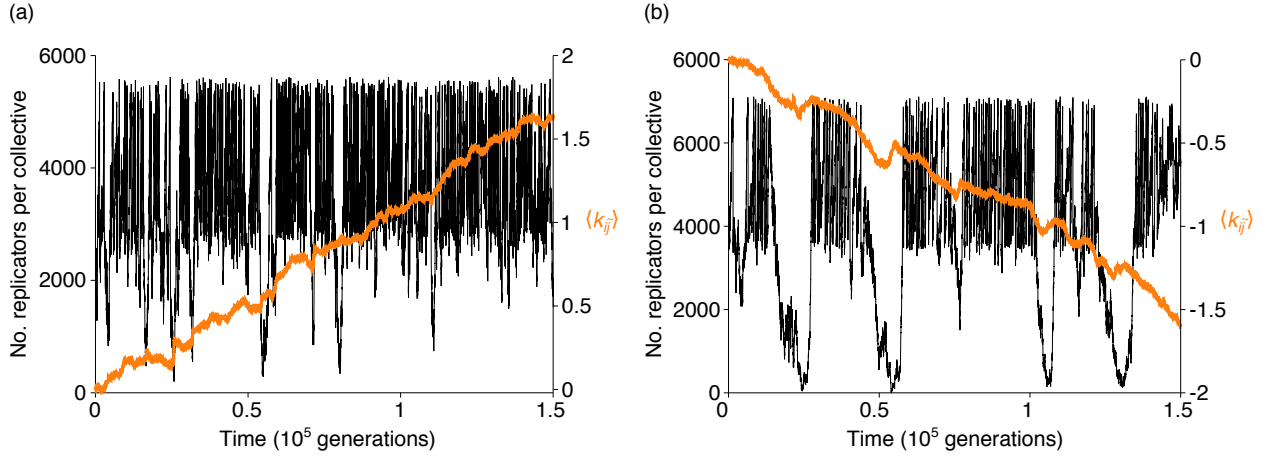


FIG. S2. Dynamics of common ancestors of collectives for $s = 0.01$ ($m = 0.01$, $M = 5 \times 10^5$ and $\sigma = 10^{-4}$). Plotted are number of replicators per collective (black; left coordinate) and $\langle k_{ij} \rangle$ (orange; right coordinate). (a) $V = 5623$. In this case, $\Delta \langle k_{ij} \rangle > 0$, and evolutionarily stable disequilibrium is not clearly observed. (b) $V = 17783$. In this case, $\Delta \langle k_{ij} \rangle < 0$, and evolutionarily stable disequilibrium is clearly observed.

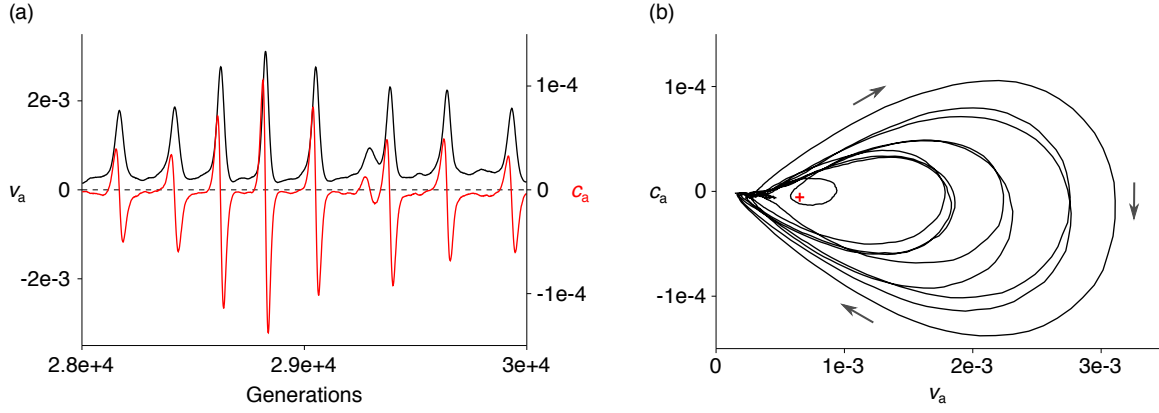


FIG. S3. Oscillation of v_a and c_a observed in simulations ($V = 5623$, $m = 0.1$, $s = 1$, $M = 5 \times 10^5$ and $\sigma = 10^{-4}$). (a) v_a (black, left coordinate) and c_a (red, right coordinate) as functions of generations. (b) Phase-space trajectory of same data as shown in a. Cross indicates mean value of v_a and c_a in this trajectory. Arrows indicate direction of trajectory.

-
- [1] L. S. Tsimring, H. Levine, and D. A. Kessler, RNA virus evolution via a fitness-space model, Phys Rev Lett **76**, 4440 (1996).